

Suppression of Chirp Interferers in GPS Using the Fractional Fourier Transform

Seema Sud

*Communication Technologies and Engineering Division
The Aerospace Corporation
Chantilly, VA 20151, USA*

seema.sud@aero.org

Abstract

In this paper we apply the Fractional Fourier Transform (FrFT) to remove chirp interferers that corrupt Global Positioning System (GPS) signals. The concept is based on the fact that in the time-frequency plane, known as the Wigner Distribution (WD), chirps are represented as lines. Using an FrFT with some rotational parameter 'a', we rotate to a new time axis t_a that transforms the chirp to a tone, in which the energy of the tone is contained in usually just one or two samples. The best 'a', and the correct time sample along the t_a axis, may be found without a priori knowledge by searching for the peak in the FrFT, since compression to one or two time samples results in an energy spike. Once the peak is found, we zero out the tone, and hence the underlying chirp. Rotation back to the original time domain via an inverse FrFT produces an improved GPS signal. This method can apply to multiple chirp interferers, and we describe how to easily determine the number of interferers, K, by finding peaks in the FrFT space over the parameter 'a'. We also describe how to easily notch the interferers once converted to tones by computing a threshold based on the power of the coarse acquisition (C/A) code and noise. We show that for signal-to-noise ratios (SNRs) greater than at least 10 dB, interferers can be notched regardless of the ratio of the C/A code power to the combined interferer power, denoted as carrier-to-interference ratio (CIR).

Keywords: Chirp, Fractional Fourier Transform, Interferer, Global Positioning System.

1. INTRODUCTION

The Fractional Fourier Transform (FrFT) is a powerful signal processing tool that has been applied to problems in the field of radar ([1], [2], [3], and [4]), communications [5], and image processing, quantum mechanics, & optics [6]. Its power comes from utilization of an entire time-frequency plane for processing signals, rather than conventional methods that use only time or frequency alone, as given by the axes on the plane. This provides numerous degrees of freedom to process signals. The FrFT was recently applied to the problem of separating multiple received target echoes in a chirp radar system [3], for example. In this paper, we propose to extend that concept to the suppression of multiple chirp interferers in GPS.

Chirp interference mitigation in GPS is a difficult problem to address because most techniques which can provide adequate interference suppression also have the negative effect of cancelling part of the desired GPS signal, since it is wideband and usually present in the same frequency bands as the interferer. In [6] the suppression of FM and some chirp-like interferers are performed with a discrete wavelet transform (DWT), but the implementation is more computationally complex and requires the interferer to be much stronger than the desired GPS signal. In [7], an amplitude domain filter (ADF) is described, but it is shown to only mitigate continuous wave (CW) interferers in GPS. In [8], the author describes an approach using an extended Kalman filter (EKF), but it too is computationally intense and is only shown to suppress FM type interferers. Finally, the authors in [9] describe a bank of pulse filters to suppress chirp interference in GPS, but their technique partially suppresses the GPS signal itself.

Approved for public release. OTR 2020-00466.

In this paper we propose an algorithm that suppresses chirp interferers effectively, over a full range of signal and interferer power levels, with minimal, almost negligible, impact to the GPS signal.

The paper outline is as follows: In Section 2, we introduce the FrFT, Section 3 presents a model of the GPS and chirp interferer signals, while Section 4 describes the proposed FrFT-based algorithm, modified from that in [3], which is applied to radar echo separation; the algorithm can suppress multiple interferers, and we discuss how to determine how many interferers are present. Simulation results are presented in Section 5, and a conclusion is given in Section 6.

2. BACKGROUND: FRACTIONAL FOURIER TRANSFORM (FrFT)

The continuous time FrFT of a function $f(x)$ of order 'a' is defined in [10]. Here, we limit our attention to discrete time and model the $N \times 1$ FrFT of an $N \times 1$ vector \mathbf{x} as

$$\mathbf{X}_a = \mathbf{F}^a \mathbf{x}, \quad (1)$$

where \mathbf{F}^a is an $N \times N$ matrix whose elements are given by ([10] and [11])

$$\mathbf{F}^a[m, n] = \sum_{k=0, k \neq (N-1+(N)_2)}^N u_k[m] e^{-j \frac{\pi}{2} k a} u_k[n], \quad (2)$$

and where $u_k[m]$ and $u_k[n]$ are the eigenvectors of the matrix \mathbf{S} defined by [11]

$$\mathbf{S} = \begin{bmatrix} C_0 & 1 & 0 & \dots & 1 \\ 1 & C_1 & 1 & \dots & 0 \\ 0 & 1 & C_2 & \dots & 0 \\ \vdots & \vdots & \vdots & \ddots & \vdots \\ 1 & 0 & 0 & \dots & C_{N-1} \end{bmatrix}, \quad (3)$$

and

$$C_n = 2 \cos\left(\frac{2\pi}{N} n\right) - 4. \quad (4)$$

The Wigner Distribution (WD) shows the energy of a signal in the time-frequency plane, just as the Fourier Transform does in the frequency domain only. It is well-known that the projection of the WD of a signal $x(t)$ onto an axis t_a gives the energy of the signal in the FrFT domain 'a', $|\mathbf{X}_a|^2$ (see e.g. [12] or [13]). In discrete time, the WD of a signal $x[n]$ is written as [14]

$$W_x\left[\frac{n}{2f_s}, \frac{kf_s}{2N}\right] = e^{j \frac{\pi}{N} kn} \sum_{m=l_1}^{l_2} x[m] x^*[n-m] e^{j \frac{2\pi}{N} km}, \quad (5)$$

where $l_1 = \max(0, n-(N-1))$ and $l_2 = \min(n, N-1)$. Aliasing is avoided by oversampling the signal $x[n]$ using a sampling rate of f_s [samples per second] that is at least twice the Nyquist rate [14].

3. SIGNAL MODEL

We assume a chirp interferer, which takes the form

$$x_k(t) = e^{j2\pi f_{d,k} t} e^{j\pi \beta_k t^2}, \quad (6)$$

where $f_{d,k}$ is the initial frequency of the chirp, k is the rate of change in the frequency in Hz/sec, and subscript k denotes the k^{th} chirp. If we now assume a scenario with a total of K interferers, we can write the composite received echo signal as

$$y(t) = ca(t) + \frac{A}{\sqrt{K}} \sum_{k=1}^K x_k(t) + \sigma_n n(t), \quad (7)$$

where the amplitude A is chosen to model a desired interference strength, of the combined K interferers, using an assumed carrier-to-interference ratio (CIR)

$$A = \sqrt{10^{-CIR/10}}. \quad (8)$$

Without loss of generality, and for simplicity, we assume the interferers all have the same amplitude in the time domain. Note that this does not mean they will have the same energies in the FrFT domain, because wider bandwidth chirps will transform to stronger tones in accordance with the energy conservation principle. Furthermore, $ca(t)$ is the desired GPS C/A code, whose amplitude is set to one. The noise $n(t)$, is modeled as additive white Gaussian noise (AWGN), whose standard deviation is set by the desired signal-to-noise ratio (SNR), using

$$\sigma_n = \frac{1}{\sqrt{2 \cdot 10^{SNR/10}}}. \quad (9)$$

The goal is to obtain the best estimate of the GPS signal, $\hat{ca}(t)$, from the received signal $x(t)$ in Eq. (7) by suppressing the K interferers, given by the summation term on the right side.

4. FRACTIONAL FOURIER TRANSFORM (FRFT) FOR CHIRP INTERFERER SUPPRESSION

The WD of a chirp signal $x(t)$, shown in Fig. 1, illustrates how the FrFT may be used to isolate chirp signals. If we rotate to the axis ' t_a ' and compute the energy in the FrFT, the chirp projects onto the axis as a strong energy tone. We can detect it by finding the peak of the energy, i.e. taking the magnitude squared of the FrFT, or $|\mathbf{X}_a|^2$ from Eq. (1). We can remove the chirp by setting the time sample at which the peak occurs, along the new ' t_a ' axis, to zero. In practice, due to the presence of the C/A signal, the energy of the noise floor will be higher; also in practice, due to motion, drift, or Doppler, the chirp may not be a perfect tone but rather will be spread out over two or more samples. We therefore require a better way to notch the interferers by computing a threshold and setting signal energy above the threshold to zero. We describe the procedure below as well as in Table I assuming a threshold, γ , and then discuss how to choose γ .

We set an index, $i = 1$, representing the first interferer to be detected based on signal strength. We search over all values of ' a ' to find the value at which the strongest chirp becomes a tone as discussed above. We first notch the tone plus some neighboring samples to compute a threshold (γ).

The threshold γ is selected by starting with the peak value that was found above. We zero out some number of samples around the peak value to eliminate the chirp, which is now a tone. Next, we find the maximum of the magnitude of the remaining signal. This is used as the threshold, and we go back to the original FrFT-domain signal and set the signal whose amplitude exceeds the threshold to zero. This was found to be the best way to only notch out only the interferer due to the following: If we simply notch the peak, we may not notch the entire chirp interferer, as it can vary slightly in frequency over time. Also, if we try to just use the signal in which some number of samples about the peak is notched, we may inadvertently notch part of the desired signal. Note

that in some application, if it is the chirp signal that is desired instead of the GPS signal, then we can simply set the signal whose amplitude is below the threshold to zero instead.

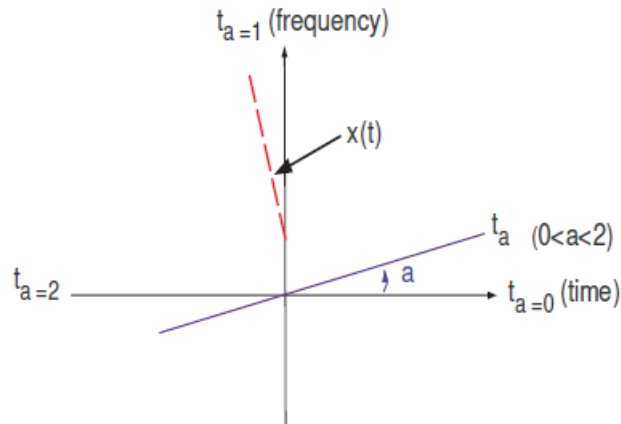


FIGURE 1: Wigner Distribution of Chirp Signal $x(t)$.

Once γ is computed, we go back to the original rotated signal and notch the tone more accurately by zeroing every sample that exceeds the threshold. After notching, we rotate back. The new time domain signal, $x_{i+1}(t)$, is an improved signal whereby the i^{th} interferer has been removed (note the use of i here instead of k because the 1^{st} interferer nulled is not necessarily the first interferer modeled). We increment i and repeat the process for all K interferers. The algorithm is presented in Table I.

Note that this method requires an estimate of how many interferers, K , are present. This can be obtained by observation of how many peaks are present in $Y_{\max,i}(a)$ in Step 1 below. This can be done by inspection, or also by computing a threshold and determining the number of peaks that fall above the threshold. The threshold would be calculated similarly to how γ is obtained above, but now we have to account for multiple peaks. For example, when two strong interferers are present, we obtain a plot such as that shown in Fig. 2, where we can clearly see that there are two strong interferers present at values of $a_{1,\text{opt}} = 1.128$ and $a_{2,\text{opt}} = 0.903$ as this is where we see peaks.

5. SIMULATIONS

In the first example, there are two chirps; the SNR is 5 dB, and the CIR is -5 dB, making the C/A code 5 dB weaker than the combined interferers. In Fig. 3 (a) and (f), we show the spectrograms of the data before and after removal of the chirps, respectively. An interesting observation that can be made from these plots is that when the CIR is negative, the interferers become stronger in power and are therefore more easily detected and notched. Upon observing the spectrum, it does not always appear that they are notched well. This is just in appearance, due to the fact that the relative power of the signal-of-interest (SOI) is initially small compared to the interferers. So even with significant interferer suppression, the SOI appears weak in the spectrogram.

We show the spectrograms of the individual interferer estimates, in Fig. 3 (b) and (d). A noteworthy point to make here is that very high frequency components in the SOI at the edges of the WD plane often get notched using this technique. This can be understood by looking back at these plots. Visualization of how the FrFT works will show that when the data is rotated to a new domain, some of the components are rotated out of the plane. Hence when the interferer is estimated, these components are included along with the interferer. Hence, they are notched as well, resulting in holes in the spectrum as can be seen in the top left and right corners of Fig. 3 (f).

The FrFTs of the received signal using the best 'a' for both chirp interferers are shown in Fig. 3 (c) and (e), respectively; we see that the FrFTs transform each chirp into a strong tone, and then

show the corresponding spectrum after the chirp (now converted into a tone) is notched; note that the tone in part (e) is the second interferer, because the first interferer has already been notched, as shown in part (c).

```

Initialize:  $i = 1$ ;  $y_i(t) = y(t)$ ;  $\delta_n = 10$ ; %  $y(t)$  is given in Eq. (7)
1. For  $a = 0 : \Delta a : 2$  % Loop over all  $a$ 
     $\mathbf{Y}(a, i) = \mathbf{F}^a y_i(t)$ ; % Compute FrFT of  $y(t)$ 
     $Y_{max}(a, i) = \max(|\mathbf{Y}(a, i)|)$ ; % Compute max value
End
2. % Find peak over all  $a$ 
    $a_{i,opt} = \arg \max_a Y_{max}(a, i)$ ;
3. % Rotate to signal  $i$ 
    $\mathbf{Y}_{peak,i} = \mathbf{F}^{a_{i,opt}} y_i(t)$ ;
4. % Compute the threshold for notching the chirp interferer
   % Store a copy of the rotated signal
    $\mathbf{Y}_{copy,peak,i} = \mathbf{Y}_{peak,i}$ ;
   % Find the index where the peak occurs in the copy
   % and set the peak as well as the  $\delta_n$  neighboring samples to zero
    $notch = \text{find}(\text{abs}(\mathbf{Y}_{peak,i}) == \max(\text{abs}(\mathbf{Y}_{peak,i}))) - \delta_n$ 
   :  $\text{find}(\text{abs}(\mathbf{Y}_{peak,i}) == \max(\text{abs}(\mathbf{Y}_{peak,i}))) + \delta_n$ ;
    $\mathbf{Y}_{copy,peak,i}(notch) = 0$ ;
   % Use the remaining signal to compute the threshold,  $\gamma$ 
    $\gamma = \max(\text{abs}(\mathbf{Y}_{copy,peak,i}))$ ;
5. % Go back to original signal in Step 3. and notch out signal  $i$ 
    $\mathbf{Y}_{peak,i} = \mathbf{Y}_{peak,i} * (\text{abs}(\mathbf{Y}_{peak,i}) < \gamma)$ ;
6. % Rotate back to  $a = 0$ 
    $y_{i+1}(t) = \mathbf{F}^{-a_{i,opt}} \mathbf{Y}_{peak,i}$ ;
7. Increment  $i = i + 1$  and repeat Steps 1-6 for  $i = 2, 3, \dots, K$ .

```

TABLE 1: Proposed Chirp Interferer Nulling Algorithm.

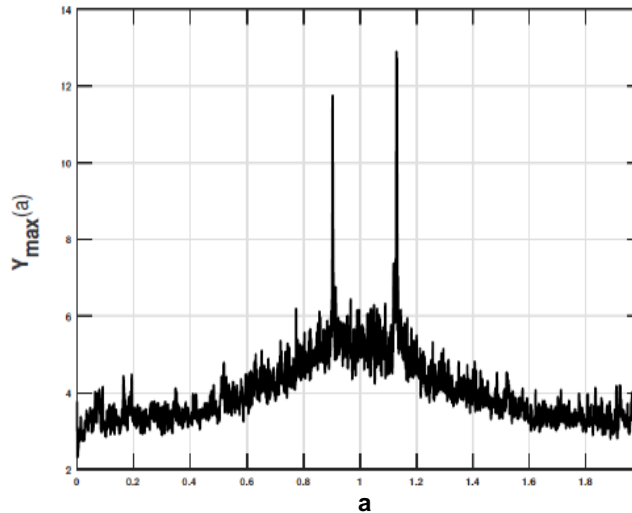


FIGURE 2: 'a' vs. $Y_{max}(a)$.

Finally, in Fig. 3 (g) and (h) we have the received signal, the true C/A bits, and the estimated C/A bits after the interferers are notched, in time and frequency space respectively. In both domains,

we can see that the chirp interferers are significantly reduced, resulting in the recovery of the GPS C/A bits. The best values of 'a' are very similar to those from the previous example. Observe from parts (f) and (h) that we are able to notch the chirp at the low frequencies more easily, as it is stronger in power here, and becomes a tone; the high frequency components, due to noise, the interferer, as well as the holes in the signal itself as explained earlier, are still present in the recovered signal. By comparing the recovered C/A signal to the original, as shown in part (g), we can compute the mean square error (MSE) to be $MSE = 0.25$.

Better nulling of interferers will occur at higher SNR. In practice, the SNR of GPS signals is usually about 30 dB or higher, and as we see with the next couple of examples, the algorithm is robust over the range of CIRs when the SNR is so high. The above example shows that it works fairly well even when the SNR is just 5 dB. This technique does not suppress noise, because the noise is distributed uniformly in the WD plane, so only a fraction of the noise appears at any value of 'a'. To null the noise would result in nulling the desired signal as well, by notching over a range of 'a'.

The next example has a single chirp interferer, so $K = 1$. We vary the interferer power using CIRs from -10 to 10 dB in steps of 5 dB. The SNR is varied from -10 to 30 dB. Typically, for GPS to operate, the SNR would be in the range of 20 to 30 dB. Fig. 4 shows the MSE between the true GPS C/A signal and that obtained from the received signal by suppressing the chirp interferer as a function of SNR, for the various CIR. When SNR is high, performance is good over all CIRs. Only when SNR becomes very low does performance degrade, due to the noise affecting the ability to compute and notch the interferer. Note that when CIR is high, this is typically when the interferer would be harder to estimate, but this is also when the signal quality is better, so estimation is less important.

Fig. 5 shows the same example but with two interfering chirp interferers, so now $K = 2$. We assume the CIR is the same for both interferers here. Performance is still robust over a range of SNRs and CIRs because the proposed algorithm can successfully find and notch independent interferers even in the presence of the pseudo-random C/A signal. There is only a slight degradation over the previous example due to the fact that when a interferer gets notched, we also notch those same frequency components in the desired SOI. Therefore, as more interferers are notched, more degradation will occur. Once again, at very low SNR, the noise dominates.

These simulations demonstrate that the proposed algorithm can adequately suppress chirp interferers in GPS over a suitably large range of SNR and CIR. The algorithm is flexible enough to operate under a range of CIR, and is able to suppress chirps that are either stronger or weaker than the GPS signal. Furthermore, the results demonstrate that degradation only occurs at low SNR (< 5 dB), but GPS signals typically operate at high SNR (> 30 dB). Suppression has minimal impact to the GPS signals themselves because only one or two samples of the GPS signal get notched for each interferer. The results also demonstrate that the algorithm can easily handle multiple chirp interferers and degrades gradually as the number of interferers increases.

6. CONCLUSION

In this paper, we describe a new algorithm that uses Fractional Fourier Transform (FrFT) to suppress chirp interferers in GPS. The FrFT converts chirps to tones, via a rotation in the time-frequency plane known as the Wigner Distribution, a useful way to view the FrFT. This operation compresses all the energy of each chirp into one or two samples, thereby increasing its energy and making interferers easy to detect and null. This process still retains the desired GPS code, because it remains spread out over the time-frequency plane and therefore only a negligible amount is nulled. The algorithm requires no prior knowledge of the nature or number of chirps because it can detect them based on energy of the rotated tones. We describe the algorithm, which notches interferers, beginning with the strongest one. We show that the algorithm is robust over a range of GPS C/A code power vs. interferer power, known as carrier-to-interference ratio (CIR). When CIR is high, the interferer may not need to be nulled; when CIR is low, the interferer is more easily detected via an FrFT, and notched. This technique can be used

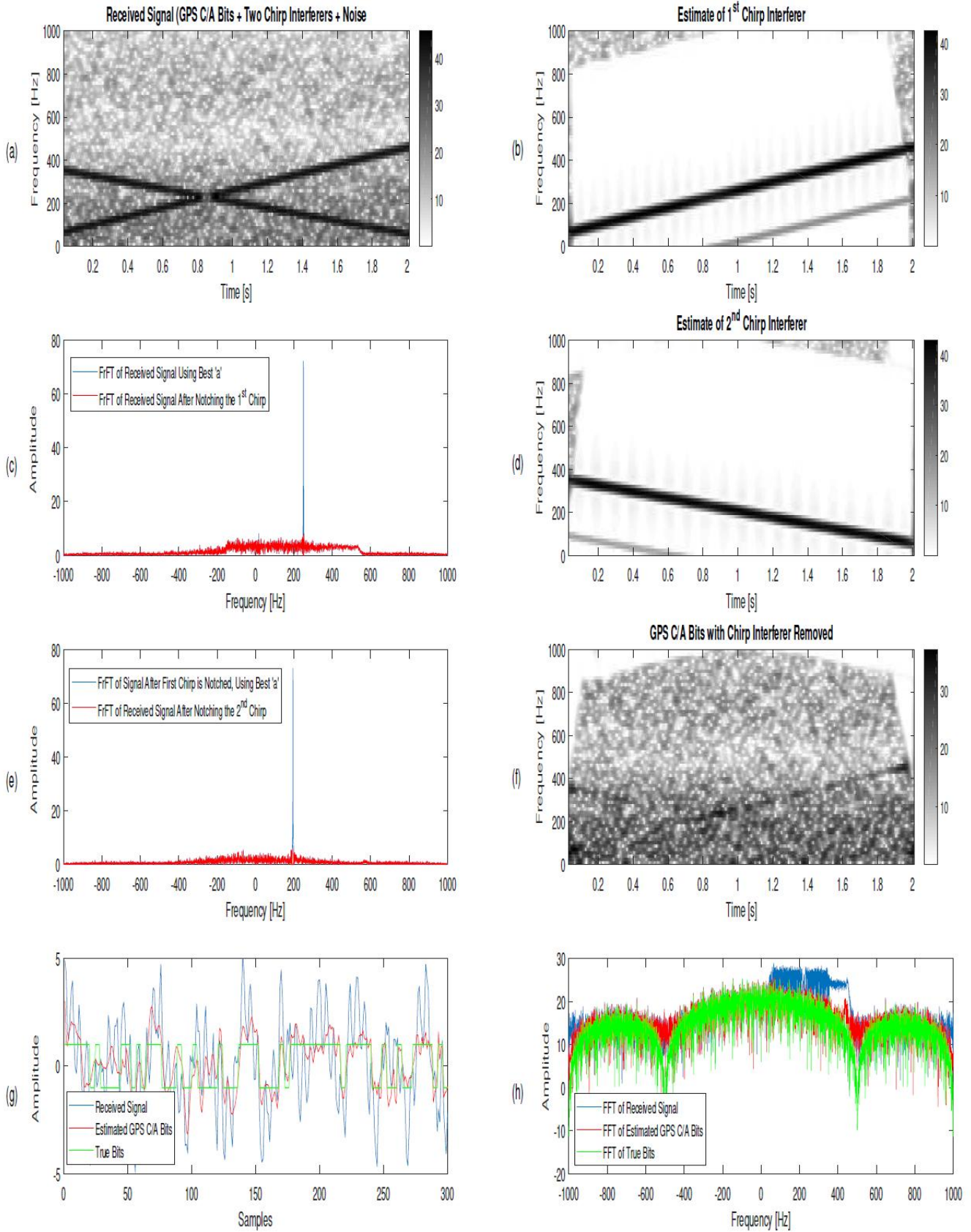


FIGURE 3: Two Chirp Interferers; SNR = 5 dB; CIR = -5 dB.

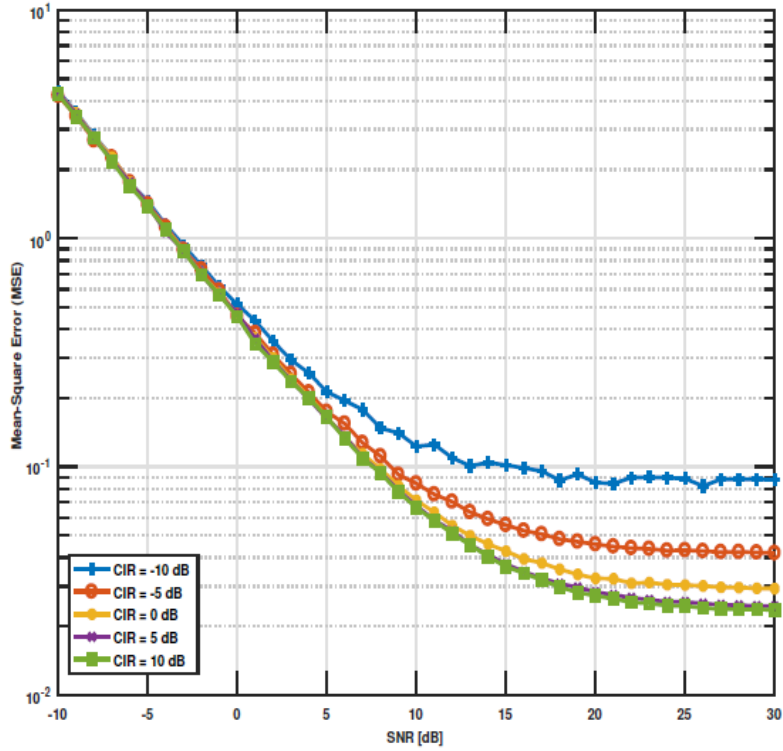


FIGURE 4: SNR [dB] vs. Mean-Square Error (MSE), K = 1 Chirp Interferer.

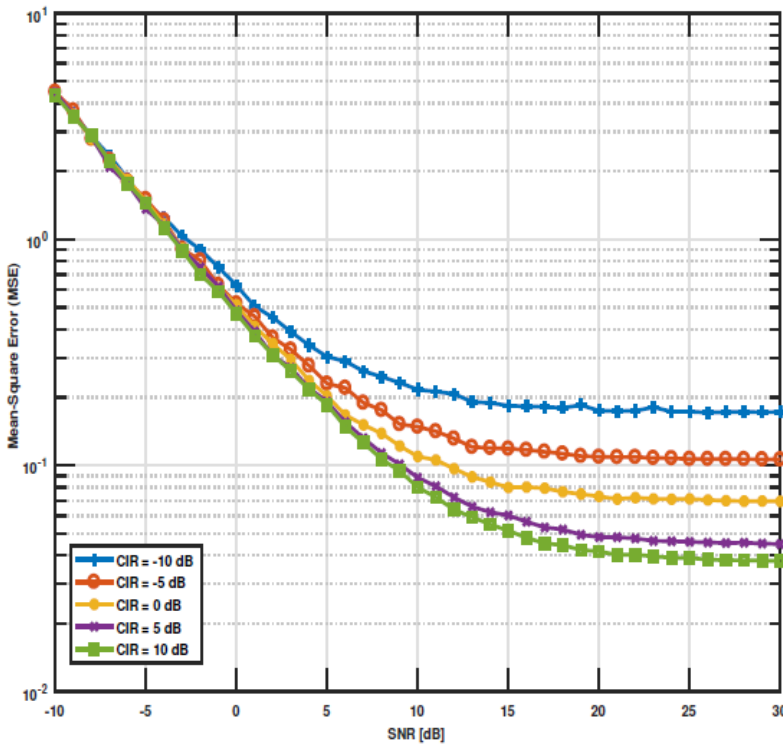


FIGURE 5: SNR [dB] vs. Mean-Square Error (MSE), K = 2 Chirp Interferers.

to remove chirp interferers in GPS. Future work includes optimizing the FrFT algorithm and testing it to ensure real-time execution is achievable, further studying the threshold for nulling the interferers, applying FrFT or other techniques to non-chirp interferers, and applying the proposed algorithm to non-GPS type signals. Developing a prototype of the algorithm in hardware and testing it with real-time GPS signals is also an area in which further development can be made.

7. ACKNOWLEDGMENTS

The author gratefully acknowledges The Aerospace Corporation for funding this work, and Alan Foonberg for helpful comments.

8. REFERENCES

- [1] H. Liu and M. Zhu, "Applying Fractional Fourier Transform to Radar Imaging of Moving Targets", Proc. IEEE Geoscience and Remote Sensing Symp. (IGARSS), Toulouse, France, Jul. 21-25, 2003.
- [2] Q. Meng and Z. Zhulin, "A New Method of Moving Targets Detection and Imaging for Bistatic SAR", Proc. IEEE 7th Int. Symp. on Computational Intelligence and Design, Hangzhou, China, Dec. 13-14, 2014.
- [3] S. Sud, "A Simple Method for Separating Weak and Strong Moving Targets in Clutter for a Radar System Using the Fractional Fourier Transform", Signal Processing: An Int. Journal (SPIJ), Vol. 10, No. 3, pp. 31-40, Oct. 2016.
- [4] H.-B. Sun, G.-S. Liu, H. Gu, and W.-M. Su, "Application of the Fractional Fourier Transform to Moving Target Detection in Airborne SAR", IEEE Trans. on Aerosp. and Electr. Systems, Vol. 38, No. 4, Oct. 2002.
- [5] S. Subramaniam, B.W. Ling, and A. Georgakis, "Filtering in Rotated Time-Frequency Domains with Unknown Noise Statistics", IEEE Trans. on Sig. Proc., Vol. 60, No. 1, Jan. 2012.
- [6] K. D. Rao and M. N. S. Swamy, "New Approach for Suppression of FM Jamming in GPS Receivers," IEEE Transactions on Aerospace and Electronic Systems, Vol. 42, No. 4, pp. 1464-1474, Oct. 2006.
- [7] R. Abimoussa and R. Landry, "Anti-jamming Solution to Narrowband CDMA Interference Problem", Canadian Conference on Electrical and Computer Engineering, Halifax, NS, Canada, Vol. 2, pp. 1057-1062, 2000.
- [8] W.L. Mao, "Novel SREKF-based Recurrent Neural Predictor for Narrowband/FM Interference Rejection in GPS", AEU Int. Journal of Electronics and Communications, Vol. 62, No. 3, pp. 216-222, Mar. 2008.
- [9] A. Rügamer, S. Joshi, Merwe, J. R. van der Merwe, F. Garzia, W. Felber, J. Wendel, and F.M. Schubert, "Chirp Mitigation for Wideband GNSS Signals with Filter Bank Pulse Blanking," Proc. of the 30th International Technical Meeting of the Satellite Division of The Institute of Navigation (ION), Portland, Oregon, pp. 3924-3940, Sep. 2017.
- [10] H.M. Ozaktas, Z. Zalevsky, and M.A. Kutay, "The Fractional Fourier Transform with Applications in Optics and Signal Processing", John Wiley and Sons: West Sussex, England, 2001.
- [11] C. Candan, M.A. Kutay, and H.M. Ozaktas, "The Discrete Fractional Fourier Transform", IEEE Trans. on Sig. Proc., Vol. 48, pp. 1329-1337, May 2000.

- [12] M.A. Kutay, H.M. Ozaktas, O. Arikan, and L. Onural, "Optimal Filtering in Fractional Fourier Domains", IEEE Trans. on Sig. Proc., Vol. 45, No. 5, May 1997.
- [13] M.A. Kutay, H.M. Ozaktas, L. Onural, and O. Arikan, "Optimal Filtering in Fractional Fourier Domains", Proc. IEEE Int. Conf. on Acoustics, Speech, and Sig. Proc. (ICASSP), Detroit, MI, Vol. 2, pp. 937-940, 1995.
- [14] J.M. O'Toole, M. Mesbah, and B. Boashash, "Discrete Time and Frequency Wigner-Ville Distribution: Properties and Implementation", Proc. Int. Symp. on Digital Sig. Proc. and Comm. Systems, Noosa Heads, Australia, Dec. 19-21, 2005.